Advanced Spray-Deposited MOD Silver Backside Metallization for Metal TIM Integration in Heterogeneous Semiconductor Packaging

Melbs LeMieux[1], Brett Walker[1], Sima Hannani[1], Kang-Yu Liu[1], Kazutaka Ozawa[1], Min-Lung Huang[2]
Yueh-Lung Lin[2], Yu-Hsun Chang[2]

Electroninks[1]
7901 East Riverside
Austin, TX, 78744
Email: Melbs@electroninks.com

Advanced Semiconductor Engineering, INC (ASE)[2]
No. 26, Jing 3rd Rd., Nanzih Dist., Kaoshiung City
811641, Taiwan (R.O.C.)

Abstract

The increasing adoption of heterogeneous integration (HI) technologies for artificial intelligence (AI), high-performance computing (HPC), and advanced radio-frequency (RF) applications has created growing demand for efficient thermal management solutions. Metal-based thermal interface materials (TIMs), including indium and pressure-less sintered silver TIMs, require robust backside metallization (BSM) to ensure reliable thermal and mechanical performance. In this work, Electroninks and Advanced Semiconductor Engineering (ASE) jointly evaluated a spray-deposited metal-organic decomposition (MOD) silver BSM technology as an additive alternative to conventional physical vapor deposition (PVD) metallization. The MOD silver films were deposited through an atmospheric spray process and characterized for morphology, conductivity, adhesion, and reliability. Integration studies with metal TIM structures demonstrated stable metallurgical bonding, low interfacial voiding, and strong interface integrity. The results establish spray-deposited MOD silver as a scalable BSM platform capable of supporting both current indium TIM and future pressure-less sintered silver TIM architectures for next-generation heterogeneous semiconductor packaging.

Key words

Heterogeneous Integration, Backside Metallization (BSM), Metal-Organic Decomposition (MOD), Thermal Interface Material (TIM), Pressure-less Sintered Silver.

I. Introduction

The rapid growth of heterogeneous integration (HI) technologies for artificial intelligence (AI), high-performance computing (HPC), and advanced radio-frequency (RF) applications has significantly increased package-level power density and thermal management requirements. Advanced packaging architectures such as chiplet integration, fan-out packaging, and embedded bridge technologies enable higher system performance but also introduce substantial thermal challenges that directly impact device reliability and operational stability [1–3].

To address these challenges, metal-based thermal interface materials (TIMs) have become increasingly important for advanced semiconductor packaging. Among various metal TIM technologies, indium-based TIM has been widely adopted in high-performance packages due to its high thermal conductivity (>80 W/m·K), excellent compliance, and proven manufacturability. More recently, pressure-less sintered silver TIM has emerged as a promising next-generation solution because of its superior thermal conductivity, high-temperature capability, and enhanced reliability for AI and HPC applications. Together, indium TIM and sintered silver TIM represent two major metal TIM architectures currently being deployed or evaluated for advanced thermal management solutions [4–6].

The performance of these metal TIM systems strongly depends on the backside metallization (BSM) layer, which serves as the critical bonding interface between the silicon die and the TIM material. Silver-based BSM is widely utilized because of its high thermal conductivity and compatibility with both indium and silver-based TIM technologies. Recent studies from leading OSAT companies have demonstrated that optimized silver BSM integrated with indium TIM can significantly improve package thermal performance. Kuo et al. reported that metal TIM integration in Fan-Out Embedded Bridge (FO-EB) packages reduced junction temperature by approximately 10°C compared with conventional silicone-based TIM while maintaining robust

reliability after thermal cycling, high-temperature storage, and uHAST testing.

Figure 1. illustrates the FO-EB thermal architecture and BSM/metal TIM development roadmap. In high-power chiplet and HBM packages, an efficient thermal path from the die backside to the heat sink is required. The BSM layer provides thermal spreading and metallurgical bonding, while the metal TIM enables heat conduction to the heat sink. This structure highlights the need for a robust, low-resistance BSM compatible with multiple metal TIM materials.

Currently, physical vapor deposition (PVD) is the dominant technology for forming BSM. While PVD provides excellent film quality and reliable metallurgical bonding with indium TIM, its dependence on vacuum processing, high capital investment, throughput limitations, and scalability challenges have motivated the search for alternative metallization approaches suitable for future heterogeneous integration platforms [7].

In this work, Electroninks and ASE jointly evaluate a spray-deposited metal-organic decomposition (MOD) silver BSM technology as an additive alternative to conventional PVD metallization. The deposited silver films were characterized in terms of morphology, conductivity, adhesion, and reliability, followed by integration studies with metal TIM architectures. This work aims to establish spray-deposited MOD Ag as a universal BSM platform capable of enabling both current indium-based TIM solutions, and future pressure-less sintered silver TIM architectures for advanced heterogeneous integration applications.

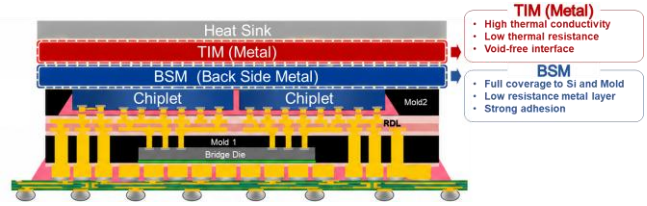


Figure 1. Schematic cross-section image of FO-EB package thermal path and development roadmap for BSM and metal TIM integration.

2. Experimental

2.1 Spray Deposited MOD Silver BSM Fabrication

A metal-organic decomposition (MOD) silver ink (**Electroninks EI-1206**) was utilized to form BSM layers on silicon substrates. Prior to coating, the silicon surface was cleaned using a standard solvent cleaning process followed by plasma surface treatment to remove organic contaminants and enhance film adhesion.

The MOD silver ink was deposited using an ultrasonic spray coating system under atmospheric conditions. Process parameters including nozzle flow rate, substrate temperature, and spray velocity were optimized to achieve uniform film coverage and target thickness. Following spray deposition with in-situ drying, the deposited films were cured to convert the MOD complex into a conductive Ag film.

2.2 Metal TIM Integration

To evaluate compatibility with advanced thermal management architectures, MOD silver BSM samples were integrated with metal TIM developed in collaboration with ASE, and two metal TIM platforms were considered, shown in **Figure 2.**

2.2.1 Indium Preform TIM Assembly

For the indium TIM route, a **97In-3Ag preform (Indium Corporation**) was positioned between the MOD silver BSM surface and the mating heat spreader. The assembly was subsequently subjected to a thermal bonding process to form the metallurgical interface. Following bonding, the resulting assemblies were evaluated for bonding quality and interfacial integrity.

2.2.2 Pressure-less Sintered Ag TIM Assembly

For the pressure-less sintered silver TIM route, a silver sintering paste (**Niching Industrial Corporation DN1206LM**) was stencil printed onto the MOD silver BSM surface. A heat spreader was then placed onto the printed paste layer using a die bonding process involving controlled temperature and bonding force to establish the desired bondline thickness and contact area. TRESKY instrument with force of 200g was employed for die bonding process. Key process parameters, including stencil thickness, heating rate, intermediate drying profile, and final sintering conditions, were evaluated through a designed experiment (DOE) approach.

The optimization focused on minimizing interfacial void formation and post-aging delamination while maintaining process stability across multiple material lots. Based on the preliminary evaluation, a pressure-less sintering condition with reduced bondline thickness and controlled thermal ramping was selected for subsequent MOD Ag BSM integration studies.

2.3 Material and Interface Characterization

The morphology and microstructure of the MOD silver BSM films were characterized using scanning electron microscopy (SEM). Film thickness was measured from cross-sectional SEM images, while electrical conductivity was evaluated using four-point probe measurements. Film adhesion was assessed according to ASTM D3359 tape testing methodology.

The interfacial microstructures formed between the MOD silver BSM and metal TIM layers were analyzed using cross-

sectional SEM and energy-dispersive spectroscopy (EDS) when applicable.

2.4 Reliability and Mechanical Evaluation

The bonding quality and reliability of the assembled structures were evaluated using scanning acoustic tomography (SAT) Tscan, cross-sectional SEM analysis, and die shear testing.

Environmental reliability evaluations included high-temperature storage testing (HTST), unbiased highly accelerated stress testing (uHAST), and thermal cycling testing (TCT). These evaluations were performed to investigate the stability of the BSM-TIM interfaces and to assess the suitability of the spray-deposited MOD silver BSM for advanced heterogeneous semiconductor packaging applications.

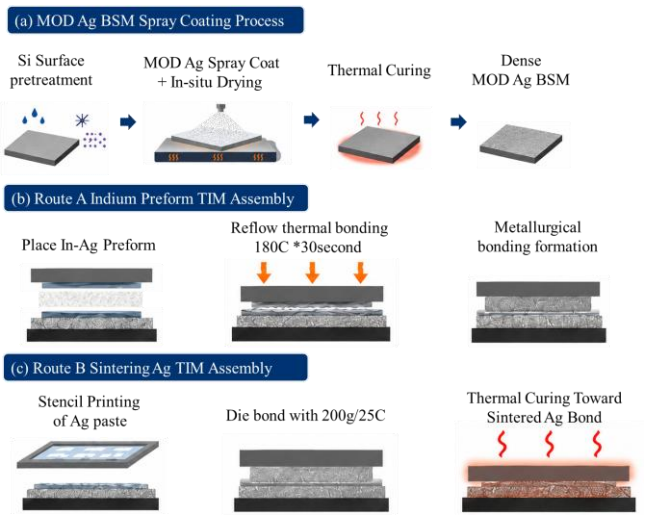


Figure 2. Process Flow for (a) MOD Ag BSM ;(b) Indium Metal TIM integration; (c) Sintering Ag TIM integration

3. Result and Discussion

3.1 Film Quality of Spray-Deposited MOD Ag BSM

The quality of the spray-deposited MOD Ag BSM was first evaluated after optimization of the drying and curing processes. Under the optimized conditions, the deposited silver film exhibited a resistivity below **50 µΩ·cm**, a surface roughness (Ra) below **0.25 µm**, and a uniform film thickness of approximately **1.7 µm**, demonstrating the capability of ultrasonic spray deposition to produce dense and uniform metallization suitable for advanced packaging applications.

Figure 3(a) presents the cross-sectional SEM image of the MOD Ag BSM deposited on an embedded bridge structure. The deposited silver layer exhibited intimate contact with both the silicon die and the surrounding epoxy molding compound without observable interfacial gaps or delamination. The conformal coverage across dissimilar materials demonstrates excellent adhesion and compatibility of the spray-deposited MOD Ag BSM with heterogeneous package structures.

The interfacial stability of the MOD Ag BSM was further evaluated through reliability testing. After exposure to **MSL3 followed by TCT-G (-40°C to 125°C)**, the silver film maintained a **5B adhesion rating** according to the cross-cut adhesion test, as shown in **Figure 3(b).** Cross-sectional SEM observations after reliability testing confirmed that the BSM thickness remained approximately **1.7 µm** and no interfacial degradation was observed.

The combination of low resistivity, smooth surface morphology, and excellent adhesion is particularly important for advanced heterogeneous integration packages, where the BSM serves as both a thermal conduction layer and the metallurgical bonding interface for subsequent metal TIM assembly. The stable adhesion observed after moisture sensitivity and thermal cycling evaluations indicates that the optimized drying and curing process successfully established a mechanically robust Ag BSM suitable for advanced packaging applications. The optimized film quality satisfied the requirements for subsequent metal TIM integration.

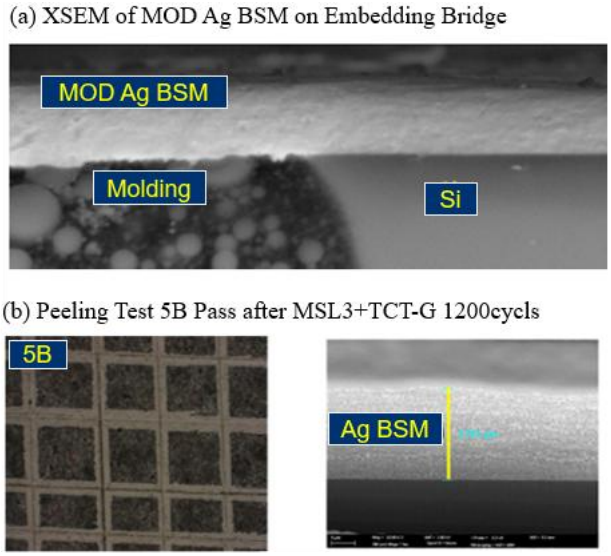


Figure 3. Characterization of the optimized spray-deposited MOD Ag BSM. (a) Cross-sectional SEM image showing conformal Ag BSM deposited across the embedded bridge structure with intimate bonding to both silicon and epoxy molding compound. (b) Cross-cut adhesion test (5B rating) after MSL3 followed by TCT-G (-40°C to 125°C), demonstrating excellent adhesion and structural integrity.

3.2 The study of the interface between MOD Ag BSM and Indium TIM

The quantitative evolution of the MOD Ag BSM/Indium TIM interface during HTST at 120°C is summarized in **Table 1**. Following TIM assembly, EDS analysis confirmed the formation of an Ag-In intermetallic layer together with indium diffusion into the MOD Ag BSM. During thermal aging, the indium concentration within the BSM increased from 52.7% to approximately 61%, while the measured Ag BSM thickness gradually decreased, indicating continued Ag-In interdiffusion and progressive interfacial reaction.

Despite the ongoing interdiffusion, the Ag BSM/IMC interface remained intact throughout the aging period. Localized voids appeared after prolonged aging, also shown in **Figure 4**; however, the overall X-ray coverage remained above 78%, indicating that significant interfacial void propagation did not occur.

In contrast, the mechanical performance exhibited a continuous decline. The average die shear strength decreased from **78.6 kgf/cm²** in the as-bonded condition to **20.2 kgf/cm²** after 125 h of aging, and the samples became **pre-detached** after 500 h. This discrepancy suggests that Mechanical integrity cannot be explained solely by interfacial void formation or metallurgical bonding evolution.

	Time 0 As-bonded	Time 125hr 120°C aging	Time 250hr 120°C aging	Time 500hr 120°C aging
Ag EDS ratio (%)	38.8	30.4	31.2	31.7
In EDS ratio (%)	52.7	62.1	60.7	61.3
BSM THK	3.53	3.67	2.09	2.39
BSM Morphology	Dense metal	*Organic formation*	*Organic sandwich*	*Organic filled*
BSM-IMC interface	Intact	Intact	*Intact but void*	*Intact with void*
X-ray Coverage %	89.33	84.20	87.13	78.74
Die shear (kgf/cm²)	78.56	*20.22*	*38.29*	*Pre-detached*

Table 1 . Aging-induced Interfacial Evolution Summary

To further understand the degradation mechanism, cross-sectional SEM observations of the MOD Ag BSM are presented in **Figure 4**. The BSM morphology evolved progressively during thermal aging, beginning with a dense metallic structure in the as-bonded condition (**Figure 4a**). Initial organic formation was observed after 125 h of aging (**Figure 4b**), followed by the development of an organic-rich sandwich structure accompanied by localized interfacial voids after 250 h (**Figure 4c**). After 500 h of aging, the BSM region became extensively filled with organic phases, and pre-detachment was observed despite the preservation of the Ag-In metallurgical interface (**Figure 4d**).

The progressive evolution of the organic-rich region closely correlates with the continuous reduction in die shear strength shown in **Table 1**. These observations suggest that the primary degradation mechanism is associated with the accumulation of organic species within the BSM region rather than loss of metallurgical bonding between the Ag BSM and the Ag-In intermetallic layer.

The origin of these organic phases is tentatively attributed to residual flux trapped during the bonding process. However, further chemical characterization, such as FTIR or ToF-SIMS analysis, will be required to verify their composition and formation mechanism. Based on this observation, future improvement of die shear performance should focus on reducing organic residue at the BSM/Indium TIM interface. Two potential approaches are being considered: fluxless bonding to eliminate flux-derived residue from the assembly process, and post-bonding defluxing to remove residual organic species when flux-assisted bonding is required. These process modifications are expected to improve the cohesive strength of the interfacial region and mitigate aging-induced die shear degradation.

The combined results from **Table 1** and **Figure 4** indicate that the reduction in mechanical strength is more closely associated with the progressive evolution of organic-rich phases than with void growth or metallurgical interface degradation.

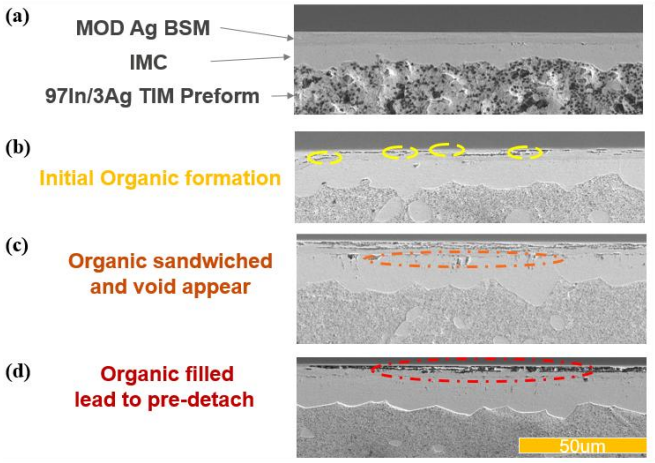


Figure 4. Progressive evolution of MOD Ag BSM morphology during HTST aging, showing the transition from a dense metallic structure to organic accumulation, sandwich formation, and eventual pre-detachment.

3.3 MOD Ag BSM Thickness Optimization for Indium TIM Integration

To investigate the influence of MOD Ag BSM thickness on interfacial diffusion behavior, EDS line-scan analysis was performed across the Ag-In bonding interface after indium TIM assembly. Representative cross-sectional SEM images and corresponding elemental line scans for BSM thicknesses ranging from approximately 3 to 10 μm are presented in **Figure 5a-5d**.

Regardless of the initial BSM thickness, indium diffusion into the MOD Ag layer was consistently confined to a limited

interfacial region. The measured indium penetration depth remained approximately **2.7–2.8 µm** for BSM thicknesses of 3, 5, and 7 µm, while only **1.6 µm** of indium penetration was observed for the 10 µm BSM because a large portion of the Ag layer remained unreacted. These observations indicate that the Ag-In reaction is diffusion-limited and localized near the bonding interface rather than extending throughout the entire BSM layer.

The diffusion-depth summary shown in **Figure 5e** further demonstrates that indium penetration does not increase with increasing BSM thickness. Instead, additional silver simply remains as residual Ag beneath the reacted region without participating in metallurgical bonding. Therefore, increasing the BSM thickness beyond the diffusion-limited reaction zone provides little additional benefit to interfacial bonding.

Combined with the nearly constant $AgIn_2$ IMC thickness observed, these results demonstrate that the Ag-In interfacial reaction is governed primarily by diffusion kinetics rather than the total silver inventory within the BSM layer. Consequently, a MOD Ag BSM thickness of approximately **3–5 µm** is sufficient to establish robust metallurgical bonding while minimizing silver consumption, reducing coating time, and lowering manufacturing cost. This finding provides a practical design guideline for industrial implementation of spray-deposited MOD Ag BSM in advanced heterogeneous integration packages.

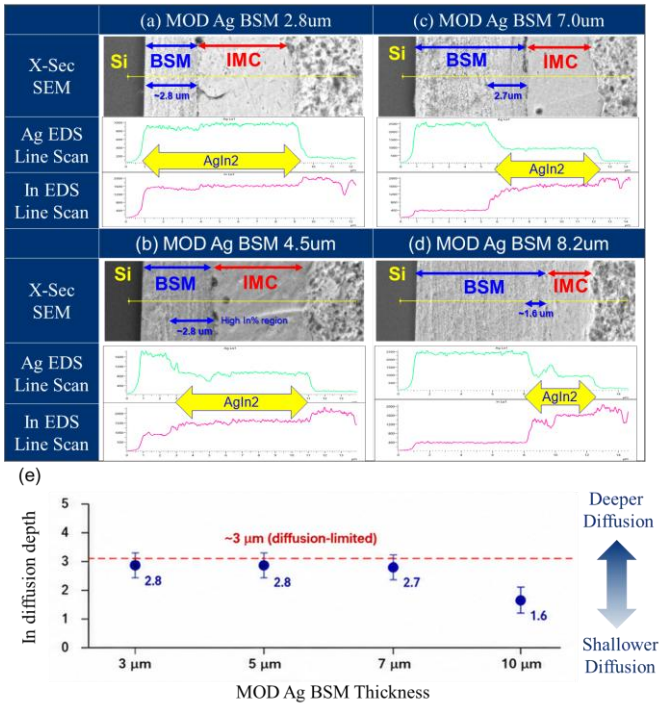


Figure 5. Cross-sectional SEM images and EDS line-scan analysis of the Ag-In interface for MOD Ag BSM thicknesses ranging from 3 to 10 µm. Indium diffusion remained confined to a ~3 µm reaction zone regardless of the initial BSM thickness, demonstrating diffusion-limited interfacial reactions.

3.4 MOD Ag BSM with Pressure-less Sintered Ag TIM Assembly

Prior process optimization identified a 100 µm stencil thickness and controlled thermal ramping profile as effective approaches for minimizing channel-type void formation during pressure-less sintering. The optimized sintering condition was subsequently adopted for all MOD Ag BSM integration experiments in this study.

The reliability performance of the pressure-less sintered Ag TIM integrated with spray-deposited MOD Ag BSM is summarized in **Figure 6.** The assemblies demonstrated excellent stability under high-temperature storage testing (HTST 150°C, 500 hr) and unbiased highly accelerated stress testing (uHAST 130°C/85%RH/33 psia, 268 hr). SAT inspection showed no significant increase in interfacial defects after reliability exposure. Cross-sectional SEM analysis further confirmed the preservation of a continuous bonding interface without observable delamination or crack propagation. Die shear strengths of 4.5 MPa and 7.4 MPa were obtained after HTST and uHAST evaluations, respectively, indicating robust metallurgical bonding and environmental stability.

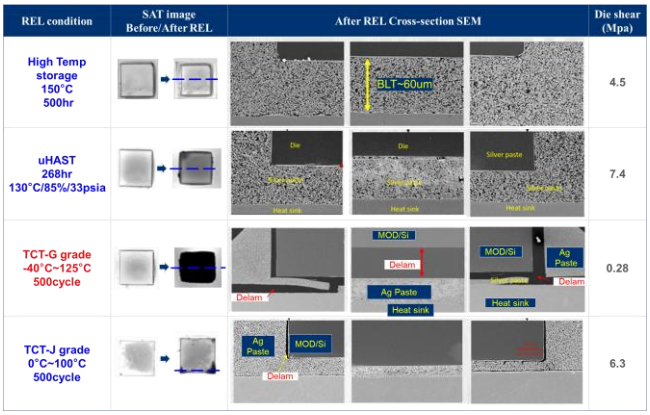


Figure 6. Reliability performance of spray-deposited MOD Ag BSM integrated with pressure-less sintered Ag TIM after HTST, uHAST, TCT-G, and TCT-J evaluations. SAT, cross-sectional SEM and die shear measurements demonstrate that thermal cycling failures originate from the die-side interface rather than degradation of the sintered Ag network.

In contrast, thermal cycling reliability revealed a strong dependence on the applied temperature range. The assemblies failed under TCT-G conditions (-40°C to 125°C, 500 cycles), where extensive delamination was observed at the die/sintered Ag interface. The measured die shear strength decreased dramatically to 0.28 MPa, confirming

severe degradation of the bonding structure. Cross-sectional SEM analysis revealed that delamination initiated preferentially at the die edge and propagated along the die/sintered Ag interface.

Unlike the indium TIM system, the dominant degradation mechanism observed for pressure-less sintered Ag TIM is associated with insufficient wetting and bonding establishment at the die-side interface during the initial assembly process rather than degradation of the sintered Ag network itself. Localized regions with inadequate wetting may have resulted in weak interfacial bonding near the die edge. Under repeated thermo-mechanical loading during thermal cycling, these weakly bonded regions acted as crack initiation sites, eventually leading to interfacial delamination. Consequently, the edge-localized failure behavior further suggests that bondline uniformity and wetting characteristics may play a more significant role than bulk sintered Ag strength in determining long-term thermal cycling reliability.

The reliability limitation of the current pressure-less sintered Ag TIM system is governed by interfacial wetting quality under thermo-mechanical cycling, rather than by the intrinsic stability of the Ag sintered network.

4. Conclusion and Future work

A spray-deposited MOD Ag backside metallization (BSM) platform was successfully developed and evaluated for metal TIM integration in heterogeneous semiconductor packaging.

For indium TIM integration, EDS analysis revealed that indium diffusion into the MOD Ag BSM was limited to approximately 3 μm regardless of the initial BSM thickness. The resulting $AgIn_2$ IMC thickness remained nearly constant across BSM thicknesses ranging from 3 to 10 μm, indicating that interfacial reactions were diffusion-limited rather than silver-limited. These results demonstrate that an optimized MOD Ag BSM thickness of 3–5 μm is sufficient to achieve equivalent metallurgical bonding performance while reducing silver consumption.

For pressure-less sintered Ag TIM integration, the MOD Ag BSM demonstrated excellent reliability under HTST and uHAST conditions. Thermal cycling failure was primarily associated with insufficient die-side wetting during initial assembly rather than degradation of the sintered Ag network itself, highlighting the importance of interfacial wetting and bondline uniformity.

Overall, the results demonstrate that spray-deposited MOD Ag BSM is compatible with both indium-based TIM and pressure-less sintered Ag TIM architectures, establishing a scalable metallization platform for next-generation heterogeneous integration applications.

Future work will focus on optimizing BSM thickness and improving die shear stability for indium TIM integration through fluxless bonding or post-bonding defluxing processes. For pressure-less sintered Ag TIM systems, future efforts will focus on improving interfacial wetting through silver powder formulation and solvent system optimization. These developments are expected to further enhance reliability and support future AI and HPC thermal management architectures.

Acknowledgment

The authors would like to thank the ASE Central R&D team for the direction of BSM development, in reliability evaluation, failure analysis, and metal TIM integration studies.

Special thanks are extended to **Niching Industrial Corporation** for their support in pressure-less sintered silver TIM material development and assembly process optimization. Their contributions were instrumental in advancing the evaluation of next-generation metal TIM architectures presented in this work.

References

[1] Garrou, P. et al., Handbook of 3D Integration, Wiley-VCH, 2014.

[2] Lau, J.H., Advanced Packaging and Heterogeneous Integration Technologies.

[3] Su, P.Y. et al., "FO-EB-T Package Solution for High Performance Computing," ECTC 2023.

[4] Chang, K.C. et al., "A Novel Indium Metal Thermal Interface Material and Package Design Configuration to Enhance High-Power Advanced Si Packages Thermal Performance," ECTC 2023.

[5] Kuo, K.H. et al., "The Study and Challenges of Backside Metal Interface Material to Enhance Fan-Out Embedded Bridge Die Package Thermal Performance," ECTC 2025.

[6] Yoon, S.W. et al., "Pressureless Silver Sintering for High Temperature Electronic Packaging Applications," Journal of Electronic Materials.

[7] Koh, Y. et al., "Thermal Performance of Advanced TIMs for High-Power FCLBGAs," ECTC 2022.